JOURNAL OF VIROLOGY, Jan. 2009, p. 552–561 Vol. 83, No. 2
0022-538X/09/$08.00+0 doi:10.1128/JVI.01921-08

The p14 FAST Protein of Reptilian Reovirus Increases Vesicular Stomatitis Virus Neuropathogenesis▽

Christopher W. Brown,[1,2]† Kyle B. Stephenson,[3]† Stephen Hanson,[3] Michael Kucharczyk,[3] Roy Duncan,[4] John C. Bell,[2] and Brian D. Lichty[3]*

Ottawa Health Research Institute, Department of Microbiology and Immunology, University of Ottawa, Ontario, Canada[1]; Department of Orthopaedic Surgery, University of Ottawa, Ontario, Canada[2]; Department of Medical Sciences, Michael G. DeGroote Institute for Infectious Disease Research, McMaster University, Hamilton, Ontario, Canada[3]; and Departments of Microbiology and Immunology and Paediatrics, Dalhousie University, Halifax, Nova Scotia, Canada[4]

Received 11 September 2008/Accepted 19 October 2008

The fusogenic orthoreoviruses express nonstructural fusion-associated small transmembrane (FAST) proteins that induce cell-cell fusion and syncytium formation. It has been speculated that the FAST proteins may serve as virulence factors by promoting virus dissemination and increased or altered cytopathology. To directly test this hypothesis, the gene encoding the p14 FAST protein of reptilian reovirus was inserted into the genome of a heterologous virus that does not naturally form syncytia, vesicular stomatitis virus (VSV). Expression of the p14 FAST protein by the VSV/FAST recombinant gave the virus a highly fusogenic phenotype in cell culture. The growth of this recombinant fusogenic VSV strain was unaltered in vitro but was significantly enhanced in vivo. The VSV/FAST recombinant consistently generated higher titers of virus in the brains of BALB/c mice after intranasal or intravenous infection compared to the parental VSV/green fluorescent protein (GFP) strain that expresses GFP in place of p14. The VSV/FAST recombinant also resulted in an increased incidence of hind-limb paralysis, it infected a larger volume of brain tissue, and it induced more extensive neuropathology, thus leading to a lower maximum tolerable dose than that for the VSV/GFP parental virus. In contrast, an interferon-inducing mutant of VSV expressing p14 was still attenuated, indicating that this interferon-inducing phenotype is dominant to the fusogenic properties conveyed by the FAST protein. Based on this evidence, we conclude that the reovirus p14 FAST protein can function as a bona fide virulence factor.

The genus *Orthoreovirus* is one of 12 accepted genera within the family *Reoviridae*, a family of icosahedral nonenveloped viruses containing a double-stranded RNA (dsRNA) genome comprised of 10 to 12 genome segments (23). Reoviruses have been isolated from a broad range of mammalian, avian, and reptilian hosts and are currently classified into five recognized species (4). Four of these five orthoreovirus species have the unusual ability to induce syncytium formation, both in infected cell cultures and in the tissues of infected animals (7, 11, 14, 34). While syncytium formation is a common cytopathic effect associated with numerous enveloped viruses, such as paramyxoviruses, herpesviruses, and retroviruses, the fusogenic reoviruses comprise the majority of examples of nonenveloped viruses with this phenotype. Relatively little is known about the role of syncytium formation in the replication cycle of the fusogenic reoviruses.

A series of recent studies have revealed the basis for the syncytium-inducing property of the fusogenic reoviruses (5, 6, 31). The four fusogenic orthoreovirus species contain an open reading frame not present in the genomes of the nonfusogenic mammalian reovirus subgroup. This open reading frame, contained within a polycistronic genome segment, encodes a small, single-pass membrane protein, and ectopic expression of this protein by itself in transfected cells results in syncytium formation (6, 31). Collectively, these different reovirus fusion-associated small transmembrane (FAST) proteins define a new family of viral membrane fusion proteins.

There are currently four members of the FAST protein family: the p10 proteins of avian reovirus and Nelson Bay reovirus, the p14 protein of reptilian reovirus, and the p15 protein of baboon reovirus, all named according to their predicted molecular mass (5, 6, 31). The p10 proteins share clear amino acid identities and an identical arrangement of structural motifs, while the p14 and p15 proteins lack sequence similarity to each other or to the p10 proteins, and each has its own unique arrangement of structural motifs. The FAST proteins do, however, share some defining structural and biological features (29). As nonstructural viral proteins, the FAST proteins play no role in reovirus entry into cells. Instead, following their expression inside virus-infected or transfected cells, the FAST proteins are trafficked to the plasma membrane in a $N_{exoplasmic}/C_{cytoplasmic}$ topology, where they induce fusion of virus-infected cells with neighboring uninfected cells. The FAST proteins are also promiscuous fusogens, fusing a wide range of different cell types. Why a nonenveloped virus would encode a dedicated, promiscuous cell-cell fusogen remains unclear.

Recent studies suggest syncytium formation may serve a dual role in the fusogenic reovirus replication cycle (29). Initially, cell-cell fusion would allow rapid localized dissemination

* Corresponding author. Mailing address: Centre for Gene Therapeutics, McMaster University, 1200 Main St., W, MDCL-5023, Hamilton, Ontario L8N 3Z5, Canada. Phone: (905) 525-9140, ext. 22478. Fax: (905) 546-9940. E-mail: lichtyb@mcmaster.ca.
† C.W.B. and K.B.S. contributed equally to this study.
▽ Published ahead of print on 29 October 2008.

of the infection while subsequent extensive syncytium formation triggers apoptosis-induced cell lysis, resulting in a burst of progeny virus release and enhanced systemic infection. This enhanced dissemination model suggests the FAST proteins could function as virulence factors, and circumstantial evidence supports this hypothesis. While the nonfusogenic mammalian reoviruses are relatively benign, the fusogenic reoviruses are pathogenic following natural infections and induce a variety of clinical symptoms. These symptoms include fatal proliferative interstitial pneumonia, subacute tracheitis, acute or fatal hepatic necrosis, and enteritis (2, 15, 17). Furthermore, there is a correlation between the extent of syncytium formation in cell culture and the pathogenicity of two natural isolates of avian reovirus (8). At present, a reverse genetics system has not been developed for the fusogenic reoviruses; therefore, it has not been possible to directly test whether the FAST proteins contribute to pathogenesis.

To further test the hypothesis that the FAST proteins can function as virulence factors, we sought to develop a recombinant virus expressing the 125-residue p14 FAST protein of reptilian reovirus (5). As a recipient virus we chose vesicular stomatitis virus (VSV), a prototypical member of the *Rhabdoviridae* family, since the pathogenesis of this virus is well characterized in mice. VSV is an enveloped negative-stranded RNA virus that buds from the plasma membrane of the infected cell and does not cause the formation of syncytia (19). VSV is spread by biting insects in subtropical regions, where it causes a relatively mild disease in farm animals characterized by lesions on the oral mucosa. When used to infect laboratory mice in experimental models, however, VSV displays a strong neurotropism and neurovirulence and can lead to lethal encephalitis, especially after intranasal administration, a characteristic not seen in cows, horses, or pigs (reviewed in reference 19). The transit of VSV into the central nervous systems (CNS) of mice has been extensively studied and has been used as a model for CNS infection, pathogenesis, and immunology (3, 13, 33). We now show that the VSV/FAST recombinant displayed normal replication in vitro but enhanced spread and neurovirulence in vivo, consistently replicating to higher titers in the brains of infected mice and mediating extensive tissue damage. The p14 FAST protein of reptilian reovirus is therefore a bona fide virulence factor that enhances viral spread in vivo.

MATERIALS AND METHODS

Generation of VSV/FAST. PCR was performed on a plasmid containing the p14 FAST cDNA using the primers CGCTCGAGACCACCATGGGGAGTGG ACCCTCTAATTTC and CGGCTAGCCTAAATGGCTGAGACATTAT CGAT in order to add an upstream XhoI site and a downstream NheI site. The resulting PCR product was cloned into the XhoI/NheI sites of pVSV-XN and pVSV-XN ΔM51. After sequencing, the genome plasmids were used to rescue infectious virus. The procedure for rescuing infectious recombinant VSV was similar to that previously described (16). Briefly, BHK cells expressing the T7 RNA polymerase (BHK-T7) were grown to ca. 85% confluence in sterile polystyrene 24-well microtiter plates (Costar catalog no. 3526). BHK-T7 cells were transfected by using Lipofectamine 2000 (Invitrogen) according to the manufacturer's protocol, with 0.5 μg of the genome plasmid and 0.5 μg of the support plasmids containing the elements of the viral ribonucleoprotein (125 ng of pBS-VSV N, 313 ng of pBS-VSV P, and 63 ng of pBS-VSV L). Rescued VSV/FAST was plaque purified three times, amplified, and titrated on Vero cells.

Viruses and cells. Vero and HEK 293T cells were obtained from the American Type Culture Collection. Cells were propagated in Dulbecco modified Eagle medium (HyClone) supplemented with 10% fetal calf serum (Cansera). BHK-T7 cells (a gift from Karl-Klaus Conzelmann) were grown in the presence of G418 (Invitrogen) at a final concentration of 0.2 mg/ml and used for virus rescues.

For production of virus used in animal experiments HEK 293T cells were infected at a multiplicity of infection of 0.01. Culture supernatants were collected 24 h later and cleared by centrifugation and filtration through a 0.2-μm-pore-size filter. Virus was pelleted and then banded on a continuous 5 to 40% sucrose gradient made in phosphate-buffered saline (PBS). Approximately 1/12 the volume of the gradient containing a visible virus band was collected and extensively dialyzed against PBS, divided into aliquots, and stored at −80°C. Stock titers were determined on Vero cells.

The ΔG VSV/RFP/FAST virus was rescued as described above except that a VSV-G expression plasmid was included in the rescue transfection. This virus was propagated on VSV-G-expressing 293 cells to provide VSV-G in *trans* and titers were determined on Vero cells by visualizing red syncytia under a fluorescence microscope.

Western blotting. Infected cells or banded virus were lysed directly in sodium dodecyl sulfate loading buffer and run on polyacrylamide gels, transferred to nitrocellulose, and blocked overnight. Blots were probed with polyclonal rabbit antibodies against VSV (a gift from Earl Brown), green fluorescent protein (GFP; Abcam), or FAST protein (5). After the blots were washed, they were probed with an Alexa Fluor 680-conjugated chicken anti-rabbit secondary antibody (Invitrogen), and the blots were then scanned on a LiCor Odyssey apparatus.

Mouse experiments. Female, 8- to 10-week-old BALB/c mice were obtained from Charles River Laboratories (Wilmington, MA). All experiments were conducted with the approval of the University of Ottawa or McMaster University Animal Care and Veterinary Services. Mice were anesthetized with 3% induction and 2% maintenance of isoflurane for intranasal instillation of 10 μl of virus and allowed to recover under oxygen. Intravenous administration of 100 μl of virus was performed through the tail vein. Mice were monitored daily and euthanized at indicated time points or upon signs of morbidity by carbon dioxide narcosis. Tissues were collected from euthanized mice and immediately placed at minus 80°C. For the in vivo biodistribution assay, single organs were halved before freezing; otherwise, only one bilateral organ was used for virus titration. The viral content of homogenized tissues was determined by plaque assay on Vero cells. All tissues had undergone only one freeze-thaw cycle, and the tissue weight was measured after homogenization.

Immunohistochemistry. Tissues were harvested as described, placed in OCT mounting media (Tissue-Tek; Sakura Finetek), and sectioned in 4-μm sections with a microtome cryostat. Sectioned tissues were fixed in 4% paraformaldehyde for 20 min and used for hematoxylin and eosin staining or immunochemistry (IHC). IHC was performed using reagents from a Vectastain ABC kit for rabbit primary antibodies (Vector Labs) according to instructions provided. Primary antibodies used were polyclonal rabbit antibodies against VSV. Briefly, endogenous peroxidase activity was blocked by incubating with 3% H_2O_2, followed by blocking of nonspecific epitopes with 1.5% normal goat serum and then blocking with avidin and biotin. PBS washes were performed between all blocking and incubating steps. Sections were incubated with anti-VSV antibody (1:5,000, 30 min), followed by anti-rabbit biotinylated secondary antibody. The avidin-biotinylated enzyme complex was added, and the antigen was localized by incubation with 3,3-diaminobenzidine. Sections were counterstained with hematoxylin. Slides were scanned on a Nikon Coolscan.

Detection of anti-VSV T cells. BALB/c mice were infected with 1e7 PFU of either VSV/GFP or VSV/FAST intravenously. Blood samples were taken 5 and 7 days postinfection, and spleens were removed at 7 days postinfection. PBMC and splenocytes were stimulated for 6 h with the N-MPYLIDFGL-C peptide (Biomer Technology), a CD8 epitope of VSV-N (25). Golgi plug (BD Bioscience) was added 2 h into the stimulation medium. Cells were then fixed; permeabilized; stained with antibodies to CD3, CD8, and gamma interferon (IFN-γ); and analyzed by flow cytometry on a FACSCanto instrument. The data were analyzed by using FlowJo software.

Determination of neutralizing antibody titers. BALB/c mice were infected with 10^7 PFU of either VSV/GFP or VSV/FAST intravenously. Blood was collected from a terminal bleed into heparin-treated Hanks balanced salt solution and centrifuged. The resulting plasma was collected, and complement was inactivated by incubating the samples at 56°C for 30 min. Each sample was then serially diluted in duplicate and incubated with 10^4 PFU of VSV/GFP for 30 min at 37°C. These neutralized samples were then transferred onto confluent Vero cells. GFP expression was analyzed on a GE Typhoon scanner 24 h later.

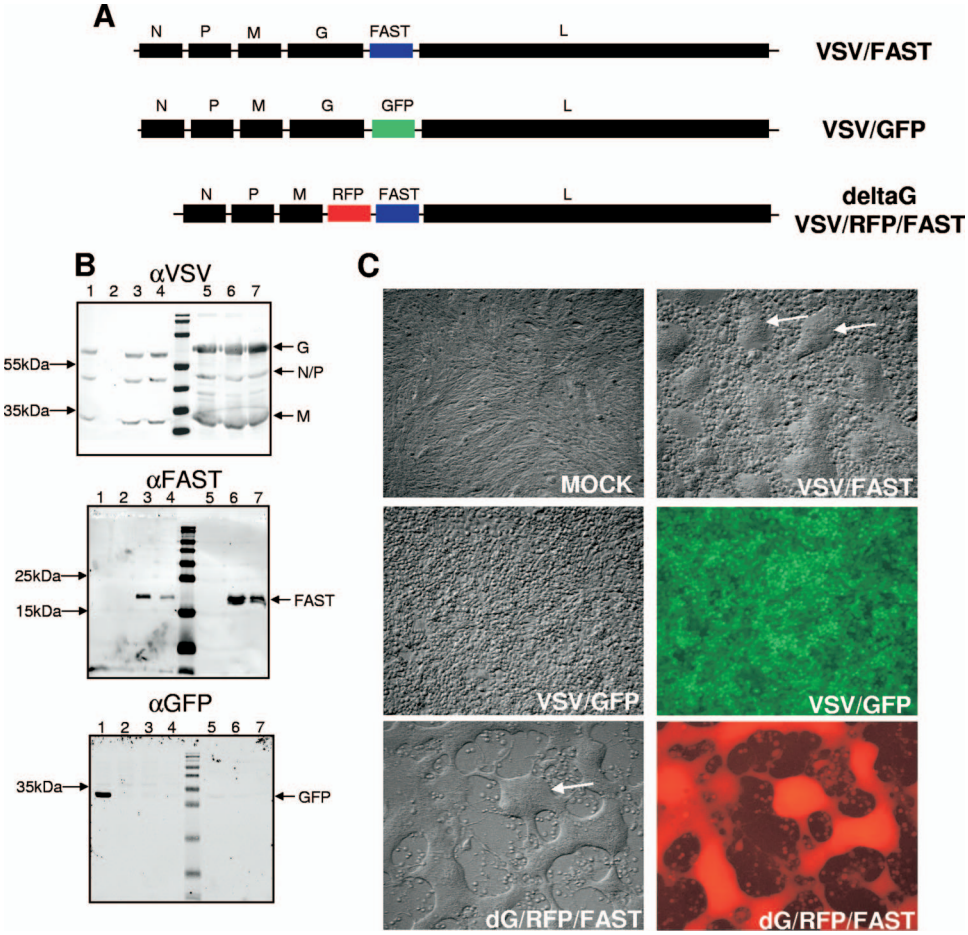

FIG. 1. Generation of VSV-FAST. (A) The p14 FAST gene from a fusogenic reptilian reovirus was subcloned into the pVSV-XN genome plasmid between the glycoprotein (G) and polymerase (L) as EGFP had been inserted previously. The G-deleted version was then made by replacing G with RFP. (B) Western blot analysis of infected cell lysates and sucrose banded virus reveals that FAST is expressed in VSV/FAST-infected cells and is present in the viral particle. Vero cells were infected with virus overnight, and cellular lysates were run (lanes 1 to 4) or virus was banded on a sucrose gradient and 10^8 PFU were run per lane (lanes 5 to 7). Blots were probed for VSV proteins (upper), FAST protein (middle), or GFP (bottom). Lanes: 1, VSV/GFP; 2, mock; 3, VSV/FAST; 4, ΔM51-VSV/FAST; 5, VSV/GFP; 6, VSV/FAST; 7, ΔM51-VSV/FAST. (C) Confluent Vero cells were infected with the indicated viruses, and photomicrographs taken 24 h later show the large multinucleated syncytia induced by the FAST viruses (arrows). Magnification, ×8.

RESULTS

Recombinant VSV expressing the p14 protein induces syncytium formation at neutral pH with no adverse effects on VSV replication. The p14 open reading frame was PCR amplified with flanking XhoI and NheI sites, and the resulting PCR product was subcloned into the corresponding sites of pVSV-XN and pVSV-XNΔM51 (Fig. 1A). The recombinant VSV/FAST and dM51VSV/FAST viruses were rescued by using standard procedures. Since recombinant VSV strains are known to be attenuated relative to parental, nonrecombinant virus (26) and insertion of additional genes into the VSV genome results altered the transcription profiles from the extended negative-strand template we therefore created the VSV/GFP recombinant to serve as the parental control, which contains the gene encoding EGFP inserted into the same location in the VSV genome as the p14 gene in VSV/FAST recombinants (Fig. 1A). The gene encoding the VSV G protein, responsible for virus attachment and virus-cell fusion during the virus entry process, was also deleted from the VSV/FAST genome and replaced with the gene encoding the red fluorescent protein (RFP) to generate the recombinant deltaG/RFP/FAST virus (Fig. 1A).

These recombinant viruses were used to infect Vero cells, and cell lysates were analyzed by Western blotting. Along with the normal repertoire of VSV proteins, the p14 protein was also expressed in cells infected with the recombinant VSV/FAST virus (Fig. 1B). Interestingly, when progeny virions from these infected cells were isolated by sucrose density gradient centrifugation, Western blotting detected the p14 protein in the same fraction containing VSV virions (Fig. 1B, top and middle panels). This was not the case for the soluble GFP protein expressed in cells infected with the VSV/GFP recombinant virus (Fig. 1B, bottom panel). The presence of p14 in the sucrose fractions containing VSV virions suggested the p14 protein might be pseudotyped onto VSV virions. Since the p14 protein possesses no receptor-binding activity and relies on cellular adhesion proteins to mediate cell binding and close

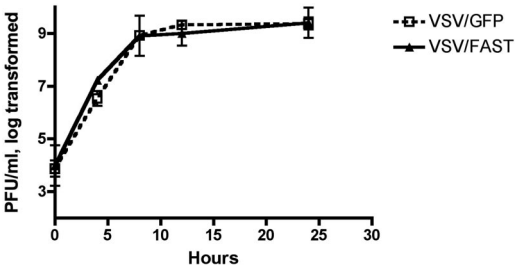

FIG. 2. Growth of VSV/FAST in vitro. Confluent monolayers of Vero cells were infected in triplicate with either VSV/GFP or VSV/FAST at a multiplicity of infection of 5.0 for 45 min in minimal medium, after which the monolayers were washed three times. Samples were collected at 0, 4, 8, 12, and 24 h postinfection, and virus titers were determined in duplicate by plaque assay on Vero cells using standard techniques. The mean of the log-transformed titers are shown ± the standard error of the mean (SEM).

membrane apposition prior to cell-cell membrane fusion (28), any p14 protein pseudotyped onto VSV virions is unlikely to affect VSV entry. This contention was supported by examining the infectivity of progeny virions released from dGVSV/RFP/FAST-infected cells. Since viruses with the G protein deleted bud from cells (22, 27, 30), progeny virions released from the dGVSV/RFP/FAST-infected cells would be lacking the VSV-G protein but might be pseudotyped with p14. These virions, however, were noninfectious, as indicated by a lack of RFP expression or syncytium formation in the recipient cultures (data not shown). Any p14 protein pseudotyped onto VSV virions is therefore unlikely to affect VSV entry.

The ability of the p14 protein expressed from the recombinant viruses to induce cell-cell fusion was confirmed by microscopy, following infection of Vero cells with the VSV/FAST virus (Fig. 1C). Efficient infection by the VSV/GFP virus, confirmed by fluorescence microscopy to detect GFP expression, resulted in no syncytia since the fusion activity of the VSV G protein is dependent on low pH activation. In contrast, the potent fusion activity of the p14 FAST protein at neutral pH was evident by light microscopy from the presence of numerous large syncytia in cells infected with either the VSV/FAST or the dG/RFP/FAST recombinants (Fig. 1C). Fluorescence microscopy confirmed infection by the dG/RFP/FAST recombinant. Similar results were obtained with HEK 293T, CT26, and BHK-T7 cells (not shown), confirming the promiscuous cell-cell fusion activity of the FAST proteins and the successful production of recombinant VSV expressing p14.

Since the recombinant VSV expressing p14 rapidly induced the formation of large syncytia in infected monolayers, and the FAST proteins have been demonstrated to induce apoptosis after cell-cell fusion (29), p14-mediated syncytium formation could impair VSV replication in vitro. This was not the case, however, since the growth kinetics of the VSV/FAST and VSV/GFP in a one-step growth curve on Vero cells were identical (Fig. 2). These results indicated that recombinant VSV containing the gene for the p14 FAST protein can be grown to high titers and that the recombinant virus possesses the cell-cell fusion activity of the fusogenic reoviruses. These recombinant viruses were used to examine the role of the p14 protein as a virulence determinant in vivo.

The p14 FAST protein increases the clinical signs of VSV neuropathogenesis. To investigate the impact of the p14 protein on VSV spread and replication in vivo, groups of five BALB/c mice were infected intranasally with a range of doses of the attenuated parental VSV/GFP or VSV/FAST recombinants. Animals were monitored for signs of hind-limb paralysis as an indicator of neuropathogenesis and euthanized at the first clear signs of paralysis. Mice developed hind-limb paralysis at day 7 postinfection with VSV/FAST at doses of 1×10^7 PFU (one of five) and 5×10^7 PFU (three of five), while at a dose of 5×10^8 three of four mice had hind-limb paralysis at day 5, and the remaining mouse developed paralysis at day 7 (Table 1). Mice receiving 1×10^7 or 5×10^7 PFU of VSV/GFP intranasally failed to develop any clinical signs of hind-limb paralysis and survived treatment. Only one of five mice receiving the highest dose of VSV/GFP developed hind-limb paralysis at 7 days postinfection. IFN-inducing mutants of VSV with a mutation in the matrix protein (ΔM51) have been shown to be highly attenuated in vivo. These viruses have mutations in the matrix protein, making them unable to block the production of IFN by infected cells (10, 32, 35). Intranasal administration of up to 10^9 PFU of a recombinant VSV carrying the p14 gene in the dM51 background (dM51VSV/FAST) resulted in no toxicity (Table 1), a dose well above the lethal dose for wild-type VSV/FAST. Thus, the fusogenic phenotype does not overcome the severe attenuation associated with IFN induction.

The p14 FAST protein increases the histopathological signs of VSV neuropathogenesis. It should be noted that in the previous experiment mice surviving infection with VSV/GFP showed no overt sequelae, while the two mice that did not develop hind-limb paralysis after infection with 5×10^7 PFU of wild-type VSV/FAST (Table 1) did not appear to recover fully. These mice both displayed weight loss, hunched posture, ruffled fur, sunken/shut eyes, erratic movement, and isolation. To further characterize the mice that survived this dose (two from VSV/FAST group and all five from the VSV/GFP group), the animals were euthanized at day 21 postinfection, and their brains were processed for histology. Histological examination of brain tissue revealed focal regions of hemorrhage and necrosis (Fig. 3). Both mice that had received VSV/FAST displayed extensive zones of cell loss extending through greater than 400 μm of tissue adjacent to the third ventricle. Immunohistochemical staining of sections adjacent to those showing histopathology detected residual VSV antigens in scattered

TABLE 1. Development of hind-limb paralysis after intranasal infection

Intranasal virus dose	Development of paralysis after infection with[a]:		
	WT-VSV/GFP	WT-VSV/FAST	M51-VSV/FAST
5×10^6	0/4	0/4	ND
1×10^7	0/5	1/5*	ND
5×10^7	0/5	3/5*	ND
5×10^8	1/5*	4/4†	0/5
5×10^9	ND	ND	0/5

[a] Values are expressed as the number of animals developing paralysis/total number of animals tested. *, Hind-leg paralysis appeared on day 7 postinfection; †, hind-leg paralysis appeared on day 5 in three cases and on day 7 in the fourth case. ND, not determined.

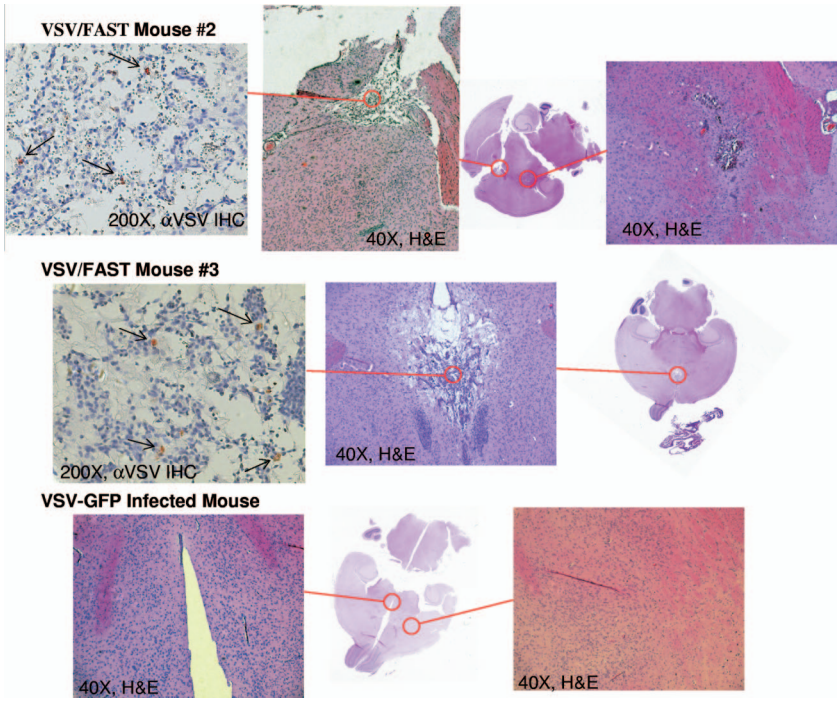

FIG. 3. VSV in the brain following intranasal administration. Of the five mice receiving 5×10^7 PFU of VSV/FAST intranasally, two failed to develop hind-limb paralysis but continued to display clinical signs (piloerection, hunched posture, etc.). These mice were euthanized on day 21 postinfection, and the brains were subjected to histological and immunohistological analysis. Sections were either stained with hematoxylin and eosin or stained with a pan-VSV polyclonal antibody. Both VSV/FAST-infected mice had large zones of damaged and inflamed tissue. Mouse 2 displayed two zones of clear damage (red circles), one of which showed a few VSV-antigen positive cells (left panel). Mouse 3 displayed one zone of clear damage that showed occasional VSV-antigen positive cells (right panel, arrows). The VSV/GFP-infected mice were also examined, and a representative section is shown, demonstrating that this obvious damage is only caused by the VSV/FAST virus. VSV antigen was undetectable in this mouse (data not shown).

cells within these lesions (Fig. 3). There was no evidence of cell loss or damage in any of the VSV/GFP-infected brains (Fig. 3), nor were residual VSV antigens detected in brain sections from mice infected with VSV/GFP stained at the same time postinfection (data not shown). Therefore, based on both clinical symptoms and preliminary histopathology, the VSV/FAST recombinant appeared to be more neuropathogenic than the corresponding parental virus not expressing the FAST protein.

To obtain further histopathological evidence that the p14 protein increases the neurovirulence of VSV, groups of five BALB/c mice were infected intranasally with 5×10^8 PFU of either the parental VSV/GFP or the VSV/FAST viruses. This dose of virus was previously shown to induce hind-limb paralysis by 5 to 7 days postinfection in 100% of the mice infected with VSV/FAST, while inducing little, if any, paralysis in mice infected with VSV/GFP (Table 1). The brains of infected animals were harvested 4 to 5 days postinfection, and serial sections were processed by immunohistochemistry using a pan-VSV antiserum to determine the extent of infection. At both time points, the extent of the zones of infection and the intensity of staining in these zones was greater in VSV/FAST-infected brains (Fig. 4). At day 4 postinfection, virus was primarily confined to the olfactory bulb in the brains of mice infected with either virus, although some sections also showed staining at distal sites (Fig. 4A and B).

By day 5 postinfection, there were notable differences observed in the immunohistochemical staining of brain tissues from animals infected with the two viruses. The staining pattern within the brains of mice infected with VSV/GFP remained largely the same as that observed at the earlier time point, with small regions of staining in the olfactory bulbs and at or near ventricles that did not extend beyond a 200-μm-thick zone (Fig. 4C, arrows in the third section). In contrast, extensive staining was seen in the middle of the brains of animals infected with the p14-expressing VSV/FAST recombinant, especially around the third ventricle (Fig. 4D). Not only was the intensity of staining stronger than that observed in VSV/GFP-infected brain tissue, but the individual foci of infection extended beyond 1,000 μm in diameter (i.e., spanning the five tissue sections examined). This enhanced intensity and greater extent of staining was seen in all VSV/FAST-infected brains. Thus, the VSV/FAST recombinant virus infected a much greater volume of brain tissue than the parental VSV/GFP virus. The immunohistochemistry results therefore provided clear evidence that the p14 FAST protein increases the ability of an attenuated strain of VSV to spread through brain tissue following intranasal infection.

The p14 FAST protein enhances the replication of VSV in the brain. Further support that the VSV/FAST recombinant is more neuropathogenic was obtained by examining the titers of infectious virus present in the brain. Groups of five BALB/c mice were infected intranasally with 5×10^7 PFU of either VSV/GFP, ΔM51VSV/GFP, or VSV/FAST. On day 6 the mice were euthanized, brains were collected, and the infectious virus

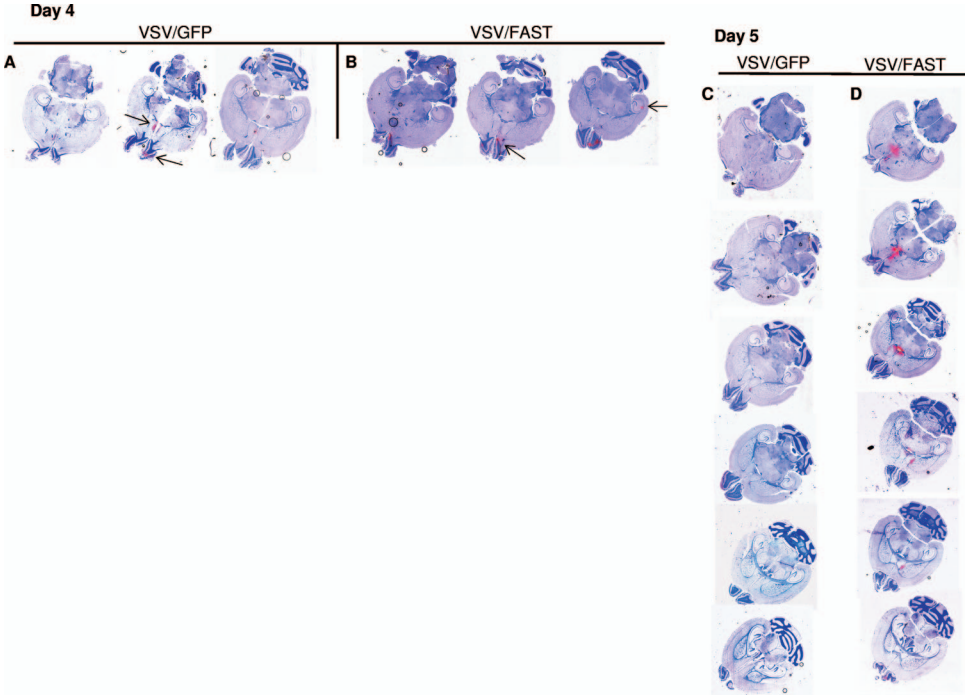

FIG. 4. Distribution of VSV/GFP and VSV/FAST in the brain after intranasal administration. BALB/c mice were infected intranasally with 5×10^8 PFU of either the parental wild-type VSV/GFP or wild-type VSV/FAST. The brains were collected for immunohistochemical staining on days 4 and 5 postinfection and stained with a pan-VSV polyclonal antibody. At day 4 postinfection virus was detected within the olfactory bulb (lower arrow, middle section, panel A), as well as in the middle of the brain (upper arrow, middle section, panel A), in brains infected with VSV/GFP, whereas the VSV/FAST virus was primarily confined to the olfactory bulb at this time point (arrow, middle section, panel B), although some brains showed staining at distal sites even at this earlier time point (arrow, rightmost section near the hippocampal sulcus, panel B). At day 5 postinfection small regions of staining were seen in olfactory bulbs at or near ventricles within the brains of mice infected with VSV/GFP (arrows, third section, panel C), while extensive staining was seen in the middle of brains, especially around the third ventricle, in mice infected with VSV/FAST (first five sections, panel D). The intensity and extent of staining observed was consistently greater in VSV/FAST-infected brains; representative brains are shown. The horizontal or axial sections shown for each brain are 200 μm apart proceeding from the bottom to the top of the brain left to right (A and B) or top to bottom (C and D).

loads were measured by plaque assay. As expected, the IFN-inducing ΔM51VSV/GFP recombinant virus failed to replicate in the brain, whereas viral replication was clearly detected in the brains of animals infected with either of the recombinant viruses containing a wild-type VSV backbone (Fig. 5). The parental VSV/GFP virus yielded highly variable virus titers at this time point, a feature we frequently observe when using this virus to infect mice (unpublished results). In contrast, all five mice infected with the VSV/FAST virus yielded consistently high titers of virus in the brain (Fig. 5), and virus isolated from the VSV/FAST-infected brains retained the syncytial phenotype in cell culture (data not shown). Although the mean tissue titers were not significantly different, the VSV/FAST-infected brains showed significantly less variation in titer since this virus consistently generated high titers after intranasal infection. The increased clinical and histopathological evidence of neuropathogenesis (Table 1 and Fig. 3 and 4) and consistently high virus titers in brain tissue (Fig. 5) all indicate that expression of the p14 FAST protein by recombinant VSV increases the neurovirulence of the virus.

The p14 FAST protein increases VSV replication in the brain following intravenous infection. To determine whether the presence of the p14 protein in VSV-infected cells could alter viral pathogenesis after infection via different routes, we exam-

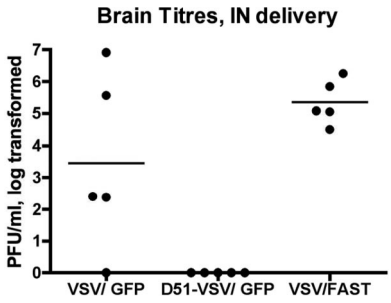

FIG. 5. VSV titers in the brain following intranasal administration. Three groups of five BALB/c mice were infected intranasally with 5×10^7 PFU VSV/GFP, ΔM51-VSV/GFP, or VSV/FAST. On day 6 brains were collected, and tissue titers were determined by duplicate plaque assays. The VSV/GFP-infected brains showed highly variable tissue titers with two brains near the limit of detection and one falling below this limit. The VSV/FAST-infected brains all showed similar, high tissue titers. Although the mean titer for the ΔM51-VSV-infected brains was significantly different than the other groups (one-way analysis of variance, $P < 0.05$), the mean titers for the VSV/GFP- and VSV/FAST-infected brains were not significantly different at this time point (one-way analysis of variance, $P > 0.05$). However, these two groups showed significantly different variances ($P = 0.0092$).

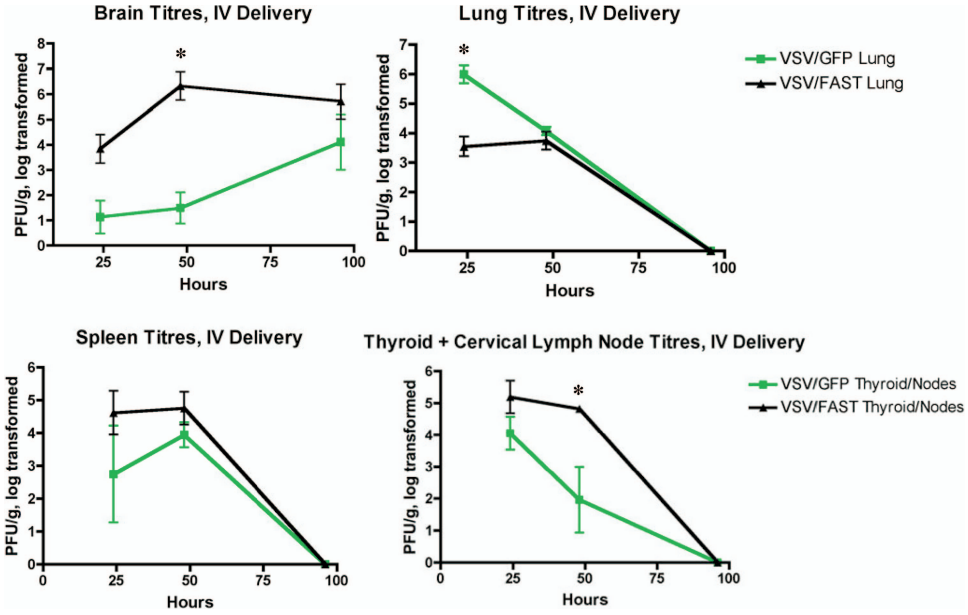

FIG. 6. Biodistribution of viruses. VSV/FAST enters the brains of mice more rapidly after intravenous infection. In two independent experiments mice were injected intravenously with 2×10^8 PFU of either VSV/GFP or VSV/FAST, and tissues from three animals were analyzed for each time point. Although in most tissues the titers measured were similar between these two viruses (i.e., the spleen shown here and data not shown), the VSV/FAST virus generated higher titers in brains and thyroid/cervical lymph nodes at the 48 h time point while showing lower titers in the lung at 24 h. At the 96-h time point virus was only detectable in brains for both viruses. Mean titers ± the SEM are shown. An asterisk (*) indicates a statistically significant difference ($P < 0.05$, two-tailed t test).

ined virus biodistribution after intravenous infection with the VSV/FAST or parental VSV/GFP recombinants. In two independent experiments, groups of three mice were injected intravenously with 2×10^8 PFU of the recombinant viruses, and the in vivo biodistribution was assessed by using a plaque assay to determine the viral load in various tissues after systemic infection. Although VSV titers increased over time in brains (Fig. 6), they declined and became undetectable by 96 h in all other tissues examined (lung, liver, spleen, heart, kidney, colon, muscle, and blood; Fig. 6 and data not shown). Although modest, the titers of VSV/FAST in tissues other than the lung were slightly elevated relative to the levels of VSV/GFP between 24 and 48 h postinfection, indicating that the VSV/FAST recombinant infects and replicates to equivalent, or slightly higher, levels compared to the parental VSV/GFP virus in numerous tissues after intravenous administration. This was not the case in lung tissue, where the titers of VSV/GFP were 3 logs higher than the titers of VSV/FAST at 24 h postinfection, declining to near-equivalent titers by 48 h postinfection (Fig. 6). It is currently unclear why expression of the p14 FAST protein in lung tissues might transiently compromise VSV replication.

In contrast to the virus yield data in these tissues, infectious virus present in the brains of animals infected with both VSV/FAST and VSV/GFP progressively increased, rather than decreased, from 24 to 96 h postinfection (Fig. 6). These results highlight the neurotropic nature of VSV. More importantly, the analysis of infectious viral yield clearly indicated a more extensive infection of the brain after the intravenous administration of VSV/FAST. At all time points tested, infectious VSV/FAST present in brain tissue was increased by 1 to 4 logs between 24 and 96 h postinfection relative to the titers obtained in animals infected with VSV/GFP (Fig. 6). In addition, hind-limb paralysis was noted in one of the three animals infected with VSV/FAST at the 96-h time point, whereas none of the VSV/GFP-infected animals demonstrated any signs of neurotoxicity by this time. Therefore, expression of the p14 FAST protein increases the neurovirulence of recombinant VSV viruses when administered via the mucosal or hematogenous routes.

Expression of the p14 protein has little, if any, effect on the immune response to VSV. Since VSV/FAST was able to cause hind-limb paralysis at lower doses than VSV/GFP in immunocompetent hosts, we sought to determine whether VSV/FAST might alter the acquired immune response to the VSV recombinants. To this end, the $CD8^+$ T-cell responses and neutralizing antibody titers induced after infection with either VSV/GFP or VSV/FAST were examined. After a single, sublethal intravenous dose of 10^7 PFU, peripheral blood was collected at 5 days postinfection, and both blood and spleens were collected at day 7 postinfection. The percentage of $CD3^+$ $CD8^+$ T cells displaying IFN-γ expression after exposure to the MP YLIDFGL nucleocapsid peptide was similar in each case (Fig. 7). The VSV/FAST-infected mice displayed approximately half the neutralizing antibody titer induced by VSV/GFP at day 7 postinfection (Fig. 8), although the titer was really only different in two of five VSV/FAST-infected mice. Thus, the recombinant VSV expressing the p14 FAST protein appears to induce a similar magnitude of T-cell response after infection and a slightly lower neutralizing antibody response.

DISCUSSION

Several enveloped viruses, such as respiratory syncytial virus, measles virus, human immunodeficiency virus, and henipavi-

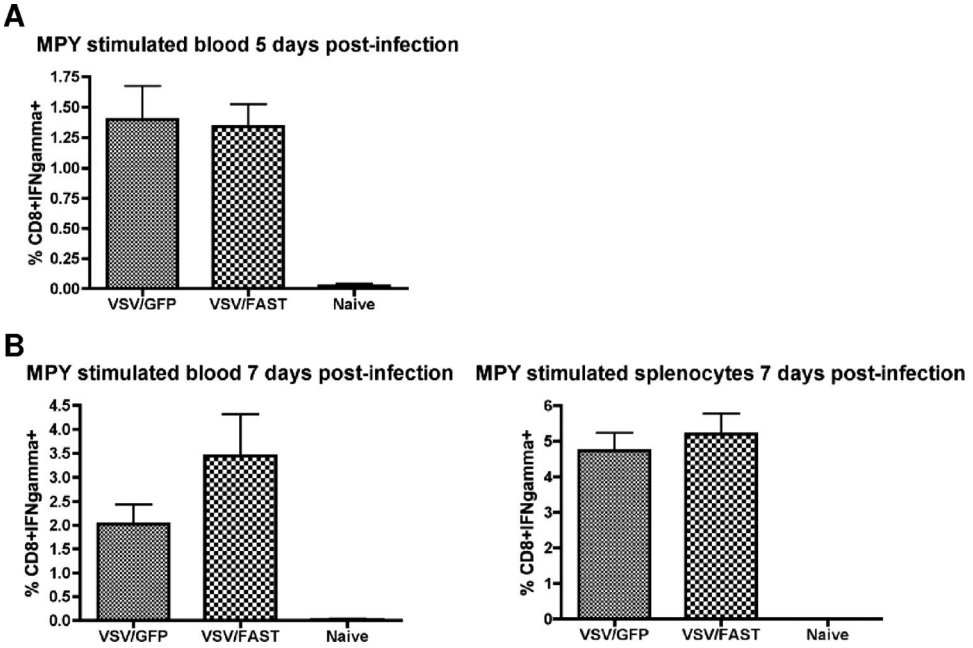

FIG. 7. $CD8^+$ T cell responses after VSV infection. Groups of five BALB/c mice were infected intravenously with 10^7 PFU of either VSV/GFP or VSV/FAST. (A) Five days postinfection peripheral blood was collected, and VSV-responsive $CD8^+$ T cells were enumerated by intracellular staining for IFN-γ production in response to the MPY peptide derived from the nucleocapsid of VSV Indiana. (B) At 7 days postinfection peripheral blood and splenocytes were collected, and VSV-responsive $CD8^+$ T cells were again enumerated. The percentages of $CD3^+$ $CD8^+$ T cells that were IFN-γ^+ after peptide stimulation ex vivo are displayed. The data shown represent the mean ± the SEM. No significant differences were detected.

ruses, induce syncytium formation in vivo. Since the viral proteins responsible for syncytium formation are also required for virus entry, it is difficult to examine the role of the syncytial phenotype in pathogenesis while excluding possible alterations in viral entry. By adding this fusogenic function to VSV, we have made a virus that does not require the syncytial phenotype for entry but utilizes this ability to enhance its spread in vivo.

In the present study we set out to determine whether or not the reoviral p14 FAST fusogenic protein can serve as a virulence factor when transferred to another, unrelated virus. To this end, we generated several recombinant strains of VSV expressing p14, in a wild-type VSV background, in an IFN-inducing mutant VSV background, and in a version with the G protein deleted. All of these viruses induced significant syncytium formation in monolayers of cultured cells in vitro. We wondered whether the rapid formation of large syncytia may lead to premature cell death and negatively impact on VSV replication; however, one-step growth curves show that VSV/FAST grows at a similar rate and to similar titers as VSV/GFP. Thus, the replication of VSV is sufficiently rapid to reach plateau prior to extensive killing of infected cells through syncytium formation.

After intranasal delivery, VSV/FAST induced hind-limb paralysis at lower doses than VSV/GFP and generated high titers of virus in the brains of these mice more consistently. We also detected enhanced replication in the CNS after intravenous administration of VSV/FAST, especially at the 48-h time point and observed hind-limb paralysis within 4 days by this route. This enhanced spread of the virus and more efficient and rapid entry into the CNS by VSV/FAST establishes the FAST fusogenic protein as a virulence factor. We do not know why the VSV/FAST virus consistently produced lower lung titers at 24 h postinfection, although one might speculate that this is the one tissue where cell death induced by syncytium formation acutely reduced VSV replication. It should also be noted that the high titers seen in brains after delivery of 5×10^7 VSV/GFP did not necessarily lead to hind-limb paralysis, while this dose of VSV/FAST usually did, despite a similar viral load in the brain. The greater brain tissue damage and clinical signs in mice that survived this dose of VSV/FAST would imply that not only does this virus enter the CNS more readily, it also does more damage once it arrives, thereby demonstrating the role of FAST as a virulence factor.

We consistently detected, after intranasal infection, VSV staining beyond the olfactory bulb at day 4 in VSV/GFP-infected brains, but we rarely detected this in VSV/FAST-infected brains (Fig. 4 and data not shown). Although the VSV/FAST virus appeared to travel into the brain more slowly by the intranasal route, the infected volume of brain and the intensity of immunohistochemical staining was always greater. After intravenous delivery, however, VSV/FAST clearly entered the brain more efficiently (Fig. 5). The formation of syncytia by this virus in the brains of mice likely leads to the greater extent of histopathology and in turn results in the increased incidence of hind-limb paralysis compared to VSV/GFP at doses that yield comparable brain tissue titers.

VSV-G is known to confer a very broad tropism; as such, it is difficult to ascertain whether the viral tropism of VSV/FAST is altered. We have observed that acid neutralization of

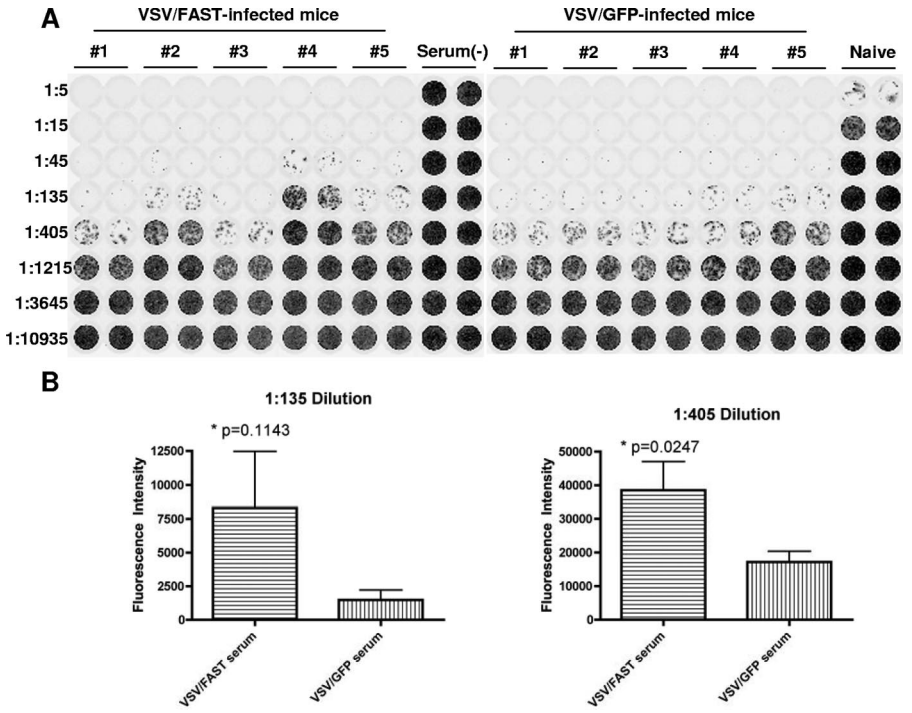

FIG. 8. VSV/FAST induces slightly lower antibody titers. Two groups of five BALB/c mice infected intravenously with 10^7 PFU of virus each. After 7 days, blood was collected into heparin-treated Hanks buffer, followed by centrifugation. The resulting plasma was collected, and complement was inactivated by incubating the samples at 56°C for 30 min. Each sample was then serially diluted in duplicate and incubated with 10^4 PFU of VSV/GFP for 30 min at 37°C. These neutralized samples were then transferred onto confluent Vero cells in 96-well plates. (A) These plates were scanned on a Typhoon scanner 24 h later to detect GFP expression (shown as black). (B) Quantification of the fluorescence intensity across each row demonstrated increased GFP intensity across the 1:135 and 1:405 dilution rows. The mean fluorescence intensity ± the SEM are shown; a statistically significant difference was detected at the 1:405 dilution (two-tailed *t* test).

VSV-G renders the VSV/FAST virus noninfectious but does not inhibit FAST-mediated cell-to-cell fusion (data not shown), indicating that the FAST protein retains its function in these conditions but is unable to mediate viral entry. In the absence of the VSV-G protein, the RFP/FAST virus was able to spread via cell-to-cell fusion; however, infectious progeny could not be propagated when filtered supernatants were passaged onto independent cell cultures, thereby supporting the notion that the FAST protein is unable to mediate viral binding and entry in the absence of G function. Furthermore, since the p14 protein possesses no receptor-binding activity and relies on cellular adhesion proteins to mediate cell binding and close membrane apposition prior to cell-cell membrane fusion (28), any p14 protein pseudotyped onto VSV virions is unlikely to affect VSV entry.

We did not detect any differences in the T-cell responses and only minor reductions in serum neutralizing antibodies after VSV/FAST infection. Based on these data, we feel that it is unlikely that the FAST protein gives this virus any significant immunoevasive properties. The infections investigated here were all of an acute nature, and in some cases the mice were reaching the endpoint prior to day 7, when a full-blown adaptive immune response would come to bear. Thus, it is unlikely that alterations in immunogenicity could explain the differences in neuropathogenesis seen between VSV/GFP and VSV/FAST.

Although it is not clear why enhanced tissue damage might benefit the reovirus from which the FAST protein is derived, this enhanced spread from the bloodstream in the infected host could help these viruses disseminate more rapidly prior to the development of an effective immune response. Alternatively, the enhanced IHC staining we observed in VSV/FAST-infected tissues may indicate that by fusing together the cytoplasm of multiple cells these viruses may have an enhanced ability to commandeer protein translation machinery. This may allow fusogenic viruses to generate more viral protein, leading to enhanced replication, especially for a virus such as reovirus that does not need to bud, since syncytia would have a reduced plasma membrane/cytoplasmic volume ratio.

The IFN-inducing mutation in the ΔM51-VSV/FAST virus attenuates toxicity in vivo and thus these fusogenic properties are not able to make VSV IFN resistant in any manner. Based on other work with this IFN-inducing mutant of VSV (1, 9, 21, 32, 36), we would predict that ΔM51-VSV/FAST will display good tumor targeting but enhanced spread in permissive tumor cells and may prove to be a superior oncolytic virus. Fusogenic viruses have also been demonstrated to have an enhanced ability to induce antitumoral immunity following oncolysis in mouse models of cancer (12, 18, 20, 24). We are currently testing our novel fusogenic VSV vector as an oncolytic therapeutic.

ACKNOWLEDGMENT

This work was funded by a grant to B.D.L. from the Canadian Cancer Society.

REFERENCES

1. **Ahmed, M., S. D. Cramer, and D. S. Lyles.** 2004. Sensitivity of prostate tumors to wild-type and M protein mutant vesicular stomatitis viruses. Virology **330:**34–49.
2. **Benavente, J., and J. Martinez-Costas.** 2007. Avian reovirus: structure and biology. Virus Res. **123:**105–119.
3. **Browning, M., C. S. Reiss, and A. S. Huang.** 1990. The soluble viral glycoprotein of vesicular stomatitis virus efficiently sensitizes target cells for lysis by $CD4^+$ T lymphocytes. J. Of Virology **64:**3810–3816.
4. **Chappell, J. D., R. Duncan, P. P. C. Mertens, and T. S. Dermody.** 2005. *In* C. M. Fauquet, M. A. Mayo, J. Maniloff, U. Desselberger, and L. A. Ball (ed.), Virus taxonomy. Eighth report of the International Committee on Taxonomy of Viruses. Elsevier Academic, San Diego, CA.
5. **Corcoran, J. A., and R. Duncan.** 2004. Reptilian reovirus utilizes a small type III protein with an external myristylated amino terminus to mediate cell-cell fusion. J. Virol. **78:**4342–4351.
6. **Dawe, S., and R. Duncan.** 2002. The S4 genome segment of baboon reovirus is bicistronic and encodes a novel fusion-associated small transmembrane protein. J. Virol. **76:**2131–2140.
7. **Duncan, R., F. A. Murphy, and R. R. Mirkovic.** 1995. Characterization of a novel syncytium-inducing baboon reovirus. Virology **212:**752–756.
8. **Duncan, R., and K. Sullivan.** 1998. Characterization of two avian reoviruses that exhibit strain-specific quantitative differences in their syncytium-inducing and pathogenic capabilities. Virology **250:**263–272.
9. **Ebert, O., S. Harbaran, K. Shinozaki, and S. L. Woo.** 2005. Systemic therapy of experimental breast cancer metastases by mutant vesicular stomatitis virus in immune-competent mice. Cancer Gene Ther. **12:**350–358.
10. **Faria, P. A., P. Chakraborty, A. Levay, G. N. Barber, H. J. Ezelle, J. Enninga, C. Arana, J. van Deursen, and B. M. Fontoura.** 2005. VSV disrupts the Rae1/mrnp41 mRNA nuclear export pathway. Mol. Cell **17:**93–102.
11. **Gard, G., and R. W. Compans.** 1970. Structure and cytopathic effects of Nelson Bay virus. J. Virol. **6:**100–106.
12. **Hoffmann, D., W. Bayer, and O. Wildner.** 2007. Therapeutic immune response induced by intratumoral expression of the fusogenic membrane protein of vesicular stomatitis virus and cytokines encoded by adenoviral vectors. Int. J. Mol. Med. **20:**673–681.
13. **Huneycutt, B. S., I. V. Plakhov, Z. Shusterman, S. M. Bartido, A. Huang, C. S. Reiss, and C. Aoki.** 1994. Distribution of vesicular stomatitis virus proteins in the brains of BALB/c mice following intranasal inoculation: an immunohistochemical analysis. Brain Res. **635:**81–95.
14. **Kibenge, F. S., and A. S. Dhillon.** 1987. A comparison of the pathogenicity of four avian reoviruses in chickens. Avian Dis. **31:**39–42.
15. **Lamirande, E. W., D. K. Nichols, J. W. Owens, J. M. Gaskin, and E. R. Jacobson.** 1999. Isolation and experimental transmission of a reovirus pathogenic in ratsnakes (Elaphe species). Virus Res. **63:**135–141.
16. **Lawson, N. D., E. A. Stillman, M. A. Whitt, and J. K. Rose.** 1995. Recombinant vesicular stomatitis viruses from DNA. Proc. Natl. Acad. Sci. USA **92:**4477–4481.
17. **Leland, M. M., G. B. Hubbard, H. T. Sentmore III, K. F. Soike, and J. K. Hilliard.** 2000. Outbreak of orthoreovirus-induced meningoencephalomyelitis in baboons. Comp. Med. **50:**199–205.
18. **Li, H., A. Dutuor, X. Fu, and X. Zhang.** 2007. Induction of strong antitumor immunity by an HSV-2-based oncolytic virus in a murine mammary tumor model. J. Gene Med. **9:**161–169.
19. **Lichty, B. D., A. T. Power, D. F. Stojdl, and J. C. Bell.** 2004. Vesicular stomatitis virus: re-inventing the bullet. Trends Mol. Med. **10:**210–216.
20. **Linardakis, E., A. Bateman, V. Phan, A. Ahmed, M. Gough, K. Olivier, R. Kennedy, F. Errington, K. J. Harrington, A. Melcher, and R. Vile.** 2002. Enhancing the efficacy of a weak allogeneic melanoma vaccine by viral fusogenic membrane glycoprotein-mediated tumor cell-tumor cell fusion. Cancer Res. **62:**5495–5504.
21. **Lun, X., D. L. Senger, T. Alain, A. Oprea, K. Parato, D. Stojdl, B. Lichty, A. Power, R. N. Johnston, M. Hamilton, I. Parney, J. C. Bell, and P. A. Forsyth.** 2006. Effects of intravenously administered recombinant vesicular stomatitis virus (VSV(ΔM51)) on multifocal and invasive gliomas. J. Natl. Cancer Inst. **98:**1546–1557.
22. **Mebatsion, T., M. Konig, and K. K. Conzelmann.** 1996. Budding of rabies virus particles in the absence of the spike glycoprotein. Cell **84:**941–951.
23. **Mertens, P. P. C., R. Duncan, H. Attoui, and T. S. Dermody.** 2005. Reoviridae. *In* C. M. Fauquet, M. A. Mayo, J. Maniloff, U. Desselberger, and L. A. Ball (ed.), Virus taxonomy. Eighth report of the International Committee on Taxonomy of Viruses. Elsevier/Academic Press, London, England.
24. **Nakamori, M., X. Fu, R. Rousseau, S. Y. Chen, and X. Zhang.** 2004. Destruction of nonimmunogenic mammary tumor cells by a fusogenic oncolytic herpes simplex virus induces potent antitumor immunity. Mol. Ther. **9:**658–665.
25. **Ramsburg, E. A., J. M. Publicover, D. Coppock, and J. K. Rose.** 2007. Requirement for CD4 T-cell help in maintenance of memory CD8 T-cell responses is epitope dependent. J. Immunol. **178:**6350–6358.
26. **Roberts, A., E. Kretzschmar, A. S. Perkins, J. Forman, R. Price, L. Buonocore, Y. Kawaoka, and J. K. Rose.** 1998. Vaccination with a recombinant vesicular stomatitis virus expressing an influenza virus hemagglutinin provides complete protection from influenza virus challenge. J. Virol. **72:**4704–4711.
27. **Robison, C. S., and M. A. Whitt.** 2000. The membrane-proximal stem region of vesicular stomatitis virus G protein confers efficient virus assembly. J. Virol. **74:**2239–2246.
28. **Salsman, J., D. Top, C. Barry, and R. Duncan.** 2008. A virus-encoded cell-cell fusion machine dependent on surrogate adhesins. PLoS Pathog. **4:**e1000016.
29. **Salsman, J., D. Top, J. Boutilier, and R. Duncan.** 2005. Extensive syncytium formation mediated by the reovirus FAST proteins triggers apoptosis-induced membrane instability. J. Virol. **79:**8090–8100.
30. **Schnell, M. J., J. E. Johnson, L. Buonocore, and J. K. Rose.** 1997. Construction of a novel virus that targets HIV-1-infected cells and controls HIV-1 infection. Cell **90:**849–857.
31. **Shmulevitz, M., and R. Duncan.** 2000. A new class of fusion-associated small transmembrane (FAST) proteins encoded by the non-enveloped fusogenic reoviruses. EMBO J. **19:**902–912.
32. **Stojdl, D. F., B. D. Lichty, B. R. tenOever, J. M. Paterson, A. T. Power, S. Knowles, R. Marius, J. Reynard, L. Poliquin, H. Atkins, E. G. Brown, R. K. Durbin, J. E. Durbin, J. Hiscott, and J. C. Bell.** 2003. VSV strains with defects in their ability to shutdown innate immunity are potent systemic anti-cancer agents. Cancer Cell **4:**263–275.
33. **Trottier, M. D., D. S. Lyles, and C. S. Reiss.** 2007. Peripheral, but not central nervous system, type I interferon expression in mice in response to intranasal vesicular stomatitis virus infection. J. Neurovirol. **13:**433–445.
34. **Vieler, E., W. Baumgartner, W. Herbst, and G. Kohler.** 1994. Characterization of a reovirus isolate from a rattle snake, *Crotalus viridis*, with neurological dysfunction. Arch. Virol. **138:**341–344.
35. **von Kobbe, C., J. M. van Deursen, J. P. Rodrigues, D. Sitterlin, A. Bachi, X. Wu, M. Wilm, M. Carmo-Fonseca, and E. Izaurralde.** 2000. Vesicular stomatitis virus matrix protein inhibits host cell gene expression by targeting the nucleoporin Nup98. Mol. Cell **6:**1243–1252.
36. **Wu, Y., X. Lun, H. Zhou, L. Wang, B. Sun, J. C. Bell, J. W. Barrett, G. McFadden, J. A. Biegel, D. L. Senger, and P. A. Forsyth.** 2008. Oncolytic efficacy of recombinant vesicular stomatitis virus and myxoma virus in experimental models of rhabdoid tumors. Clin. Cancer Res. **14:**1218–1227.